



Dielectric confinement in quantum dots of arbitrary shape within the local spin density approximation: Diluted regimes in elongated quantum dots

J. L. Movilla, M. Pi, and J. Planelles

Citation: *J. Appl. Phys.* **108**, 064311 (2010); doi: 10.1063/1.3487479

View online: <http://dx.doi.org/10.1063/1.3487479>

View Table of Contents: <http://jap.aip.org/resource/1/JAPIAU/v108/i6>

Published by the American Institute of Physics.

Related Articles

Tetrahedral chalcopyrite quantum dots for solar-cell applications
Appl. Phys. Lett. **99**, 111907 (2011)

Optical routing and switching of energy flow in nanostructure systems
Appl. Phys. Lett. **99**, 113113 (2011)

Excitations in doped quantum dot induced by accelerating impurity center
J. Appl. Phys. **110**, 054314 (2011)

Symmetry reduction in multiband Hamiltonians for semiconductor quantum dots: The role of interfaces and higher energy bands
J. Appl. Phys. **110**, 053710 (2011)

Compositional effects on the electronic structure of ZnSe_{1-x}S_x ternary quantum dots
Appl. Phys. Lett. **99**, 101902 (2011)

Additional information on *J. Appl. Phys.*

Journal Homepage: <http://jap.aip.org/>

Journal Information: http://jap.aip.org/about/about_the_journal

Top downloads: http://jap.aip.org/features/most_downloaded

Information for Authors: <http://jap.aip.org/authors>

ADVERTISEMENT



Submit Now

Explore AIP's new open-access journal

- Article-level metrics now available
- Join the conversation! Rate & comment on articles

Dielectric confinement in quantum dots of arbitrary shape within the local spin density approximation: Diluted regimes in elongated quantum dots

J. L. Movilla,¹ M. Pi,² and J. Planelles^{1,a)}

¹Departament de Química Física i Analítica, Universitat Jaume I, Box 224, E-12080 Castelló, Spain

²Departament ECM, Facultat de Física and IN² UB, Universitat de Barcelona, E-08028 Barcelona, Spain

(Received 23 June 2010; accepted 6 August 2010; published online 21 September 2010)

We propose a simplified and computationally feasible model accounting for the dielectric confinement in arbitrarily shaped many-electron quantum dots, within the local spin density approximation. The model yields quite a good agreement with full configuration interaction calculations including exact dielectric confinement. The model is used to study the influence of the dielectric confinement on the electronic charge distribution of elongated quantum dots in the low density regime. © 2010 American Institute of Physics. [doi:10.1063/1.3487479]

I. INTRODUCTION

According to the electrodynamics of continuous media, when electrons are confined in a quantum dot (QD) embedded in a dielectrically mismatched matrix, surface polarization-induced charges appear.¹ The effect of the dielectric mismatch is relevant, for it may lead to unexpected behavior and challenges in the implementation of devices in nanoelectronics,² but also constitutes a tailoring tool of pursued physical responses,³ having proved to be the driving mechanism to explain experimental observations such as the large variation in the optical gap of CdSe nanorods (NRs) compared to the transport one,⁴ or the large magnitude of the polarization anisotropy on linear^{5–7} and nonlinear⁸ optical phenomena. The influence of the image charges on the electronic structure of homogeneous spherical QDs is described in the pioneering papers by Brus.⁹ As mentioned, a proper account for the effects stemming from the dielectric mismatch between the QD and its surroundings, also called dielectric confinement, has been proved of utmost relevance in the agreement between theoretical predictions and experimental observations.^{4,10} Two new terms arise in the Hamiltonian due to the dielectric confinement. On the one hand, there is a single-particle contribution coming from the interaction of carriers with their own induced charges (self-polarization potential), and, on the other hand, there are two-particle contributions coming from the interaction of a carrier with the charge induced by the other one (polarization of the Coulomb interaction). The calculation of the self-polarization potential is really involved, even in the case of electrons confined by finite barriers in spherically symmetric QDs.^{11,12} Very recently, a new numerical method revealed good performance extending the calculations to dielectric spheroids.¹³ The further extension to axially symmetric QDs, such as lens, cylindrical or ring shaped QDs, has also been published this year.¹⁴ The proposed computational scheme, that can be easily extended to irregularly shaped QDs, relies on the numerical calculation of the image charges induced by

the carriers at the dielectric interface.^{15,16} The calculation of the polarization of the Coulomb interaction requires computing the image charges induced by a given electron density distribution. All the same, the calculation of the self-polarization potential is much heavier and involved, as it requires a series of calculations of image charges produced by an electron which is being located in each node of the discretization grid, thus breaking the axial symmetry. Strategies enabling an efficient achievement of convergence in the calculation of the self-polarization potential of QDs embedded in dielectric media are detailed in the abovementioned paper.¹⁴ However, large-scale linear systems solvers using secondary storage are needed for self-polarization potential calculations of recently synthesized hybrid QDs composed of a semiconductor trunk connected to one or two metal-like tips, the whole structure being generally buried in an insulating medium.^{17,18}

When the number of electrons in a QD is small, one can proceed to account for dielectric mismatch and carry out the most rigorous, and computationally very demanding, full configuration interaction (FCI) calculations.^{19,20} However, larger systems require less-demanding methods, such as the density functional theory (DFT).²¹ The practical limitations of this method come from the not exactly known exchange-correlation potential, but the general experience is that DFT results are quite reliable,²² and they have contributed substantially to an understanding of QD electronic structure and addition spectra.^{23,24} Some of us proposed a DFT scheme, within the local spin density approximation (LSDA), which accounts for the dielectric confinement in many-electron spherical QDs.²⁵ In this approach, the self-polarization potential is separately calculated and injected into the Kohn-Sham²⁶ Hamiltonian as a second confining potential, while the Coulomb functional is accounted for by solving the Poisson equation in dielectric media. Finally, both exchange and correlation functionals were modified by means of proper scaling factors. The extension of this approach to arbitrarily shaped QDs, although desirable, reveals a difficult implementation. In this paper, we propose a simplified and feasible model to account for dielectric confinement in

^{a)}Electronic mail: josep.planelles@qfa.uji.es.

LSDA for irregularly shaped QDs. For the sake of computing simplicity, we will show results on axially symmetric systems.

II. THEORY

A. Framework methodology

The LSDA is a well-known approach, fully developed in several papers and books, as, e.g., Ref. 21. A brief outline may be found in, e.g., Sec. II of Ref. 25. Then, for the sake of brevity, we will not sketch it now. We though summarize next the induced charge calculation. It is based on the fact that the Coulomb Potential $\Psi(\mathbf{r})$ generated by a charge distribution $\rho(\mathbf{r})$ in an inhomogeneous dielectric medium, obtained by solving the generalized Poisson equation,

$$\nabla[\epsilon(\mathbf{r}) \nabla \Psi(\mathbf{r})] = -4\pi\rho(\mathbf{r}), \quad (1)$$

where $\epsilon(\mathbf{r})$ is the position-dependent dielectric constant, can also be expressed as a sum

$$\Psi(\mathbf{r}) = \Psi_s(\mathbf{r}) + \Psi_i(\mathbf{r}), \quad (2)$$

with $\Psi_s(\mathbf{r})$ and $\Psi_i(\mathbf{r})$ fulfilling

$$\nabla^2\Psi_s(\mathbf{r}) = -4\pi\rho(\mathbf{r}), \quad (3)$$

$$\nabla^2\Psi_i(\mathbf{r}) = -4\pi h(\mathbf{r}), \quad (4)$$

i.e., the potential generated in a vacuum by the real charge $\rho(\mathbf{r})$ plus the one generated by the induced charge $h(\mathbf{r})$.

Substituting Eqs. (2)–(4) in Eq. (1), and after some algebra, we have,

$$\epsilon(\mathbf{r})h(\mathbf{r}) = [1 - \epsilon(\mathbf{r})]\rho(\mathbf{r}) + \frac{1}{4\pi} \nabla \epsilon(\mathbf{r}) \nabla [\Psi_s(\mathbf{r}) + \Psi_i(\mathbf{r})]. \quad (5)$$

We obtain $\Psi_i(\mathbf{r})$ by numerically discretizing Eq. (5). Details may be found in Ref. 14.

In order to account for the dielectric effects in LSDA we propose the model we describe in Sec. II B, that basically consists in supplementing the external potential of the Kohn–Sham LSDA Hamiltonian by the Coulomb potential produced by the charge $h(\mathbf{r})$ induced in the inhomogeneous dielectric medium by the real charge distribution $\rho(\mathbf{r})$.

B. The model

The model is based on the following idea. Suppose that a static charge distribution is embedded in a homogeneous dielectric medium. If this medium is replaced by an inhomogeneous one, then, the charge density distribution rearranges to reach equilibrium in this new medium. Since the influence of the inhomogeneous medium may be replaced by a set of image charges in a vacuum, we may imagine the fulfillment of the final equilibrium as a set of iterative steps starting from an unperturbed charge distribution $Q^{(0)}$. As a first step, this unperturbed real charge distribution induces a given virtual charge distribution $IC^{(0)}$. We then fix $IC^{(0)}$ and allow the real charge, under the influence of $IC^{(0)}$, to reach a new equilibrium distribution $Q^{(1)}$. The new real charge distribution

$Q^{(1)}$ yields a new induced charge distribution $IC^{(1)}$. The process is repeated until convergence ($Q^{(i+1)} \approx Q^{(i)}$).

We implement this idea in the self-consistent Kohn–Sham scheme. We start by solving the LSDA problem of a many-electron QD embedded in a homogeneous medium. Then, we obtain a set of occupied spin up and down orbitals that define a total electron density distribution. We call it $Q^{(0)}$ and proceed to the induced charge computation $IC^{(0)}$ as described in Ref. 14. Then, we consider the potential produced by the induced charge as an extra external potential to be included in the Kohn–Sham Hamiltonian and proceed to iterate, thus reaching a new set of occupied spin up and down orbitals that define a new total electron density distribution $Q^{(1)}$. In turn, $Q^{(1)}$ induces $IC^{(1)}$, and the process is repeated until convergence. Note that $IC^{(n)}$ includes both, self-polarization of each electron and polarization of the Coulomb interaction.

The proposal is computationally feasible and gives quite a good agreement with FCI calculations including dielectric confinement, as we show in Sec. III.

III. METHOD VALIDATION AND ILLUSTRATIVE CALCULATIONS

Our first goal in this section is to validate the proposed method for the study of the electronic density structure in diluted regimes, where the Coulomb effects of the dielectric mismatch are expected to be of greatest significance. We assume a CdSe (dielectric constant $\epsilon=9.2$ and effective mass $m^*=0.13$) colloidal NR composed by a cylinder of radius $R=2$ nm and length L attached to two hemispherical caps of the same radius, surrounded by a medium with dielectric constant ϵ_{out} . The confining potential presents a misalignment of 4 eV between the rod and its surroundings, and, for coherence with the dielectric model, displays a cosinelike profile within a 0.5 nm width interfacial region. We carry out LSDA together with FCI calculations for $L=9$ nm, assuming in both cases an insulating surrounding medium ($\epsilon_{\text{out}}=2$) and a surrounding medium of the same dielectric constant as the rod ($\epsilon_{\text{out}}=9.2$). The FCI program used is the same as in Ref. 27. As in such a paper, a basis set ensuring saturation along the NR axis is employed. In the presence of dielectric mismatch, the evaluation of the corresponding Coulomb matrix elements goes through a similar induced charge computation as the one we employ in the LSDA model.

Figure 1(a) shows the N -electron ground state densities along the rod axis (ρ_z) obtained for $N=4$ and 6 in the absence of dielectric mismatch. In both cases the system presents a charge density wave (CDW), characterized by $N/2$ maxima in the density profile. As observed, the LSDA results are in qualitative agreement with the FCI ones, though FCI densities seem to show a bit larger electron correlation, which is observed by the appearance of deeper valleys and more separated maxima.²⁸

The agreement is more apparent when the dielectric polarization is taken into account [Fig. 1(b)]. The CDW phase obtained previously is preserved in both cases ($N=4$ and 6), the main difference being an increased concentration of the

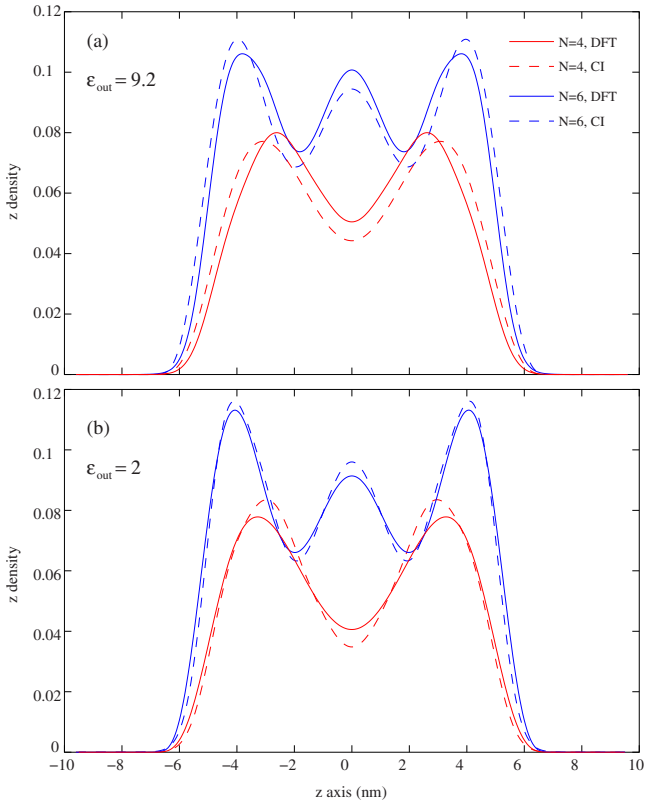


FIG. 1. (Color online) LSDA (solid) and FCI (dashed) electronic density profiles along the rod axis (ρ_z) for a $L=9$ nm CdSe rod populated with $N=4$ (curves showing two maxima) and $N=6$ (curves showing three maxima) and for (a) $\epsilon_{\text{out}}=\epsilon_{\text{rod}}=9.2$ and (b) $\epsilon_{\text{out}}=2$.

electron density in the rod ends as compared to $\epsilon_{\text{out}}=9.2$. This dielectric effect has already been reported for similar $N=2$ electron NRs.²⁰

Let us next use the LSDA method presented to reach much more diluted regimes which are beyond the reasonable possibilities of the FCI method.³⁰ In the following, and in order to enhance the dielectric mismatch effects to its maximum, we will assume a value of $\epsilon_{\text{out}}=1$ to describe the insulating medium.

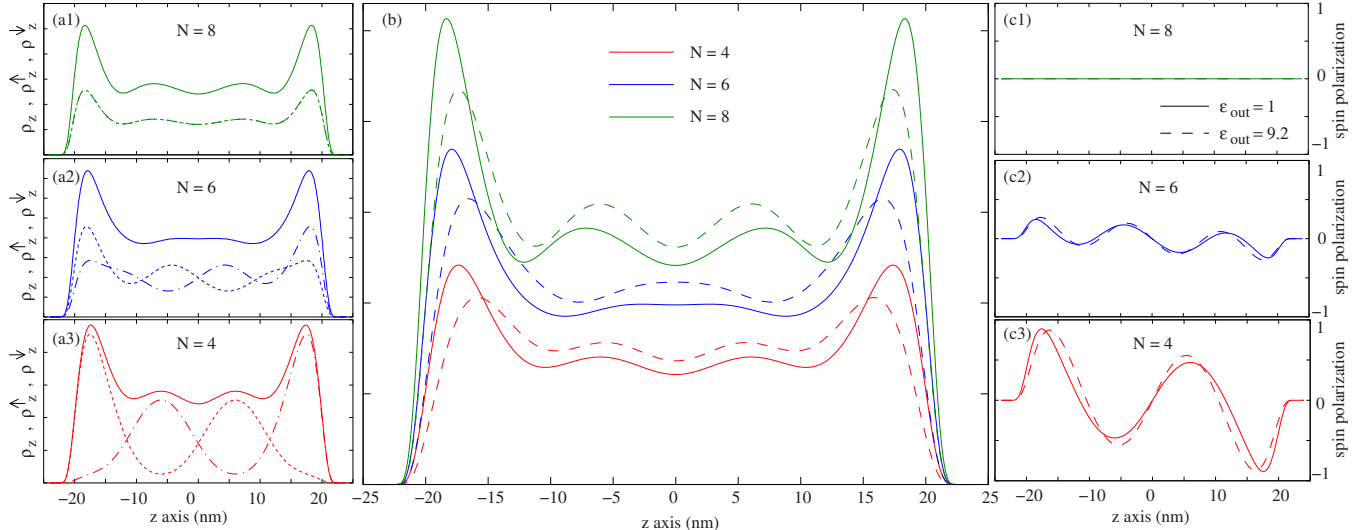


FIG. 2. (Color online) [(a1)–(a3)] ρ_z (solid), ρ_z^{\uparrow} (dotted), and ρ_z^{\downarrow} (dash dotted) densities for a $L=40$ nm CdSe rod immersed in a $\epsilon_{\text{out}}=1$ dielectric medium and populated with $N=8, 6$, and 4 electrons. (b) ρ_z profiles for the studied cases assuming $\epsilon_{\text{out}}=1$ (solid lines) and $\epsilon_{\text{out}}=9.2$ (dashed lines). [(c1)–(c3)] Normalized spin polarization $[(\rho_z^{\uparrow} - \rho_z^{\downarrow})/\max(\rho_z)]$ for the studied cases assuming $\epsilon_{\text{out}}=1$ (solid lines) and $\epsilon_{\text{out}}=9.2$ (dashed lines).

We plot in Fig. 2 the electronic charge density (ρ_z) and the spin up and down densities (ρ_z^{\uparrow} and ρ_z^{\downarrow}) corresponding to a $L=40$ nm rod with different electron populations and for $\epsilon=9.2$ and $\epsilon_{\text{out}}=1$. In this regime of electron dilution, the $\epsilon_{\text{out}}=9.2$ system presents for $N=4$ a spin density wave (SDW) phase (not shown), with broken spin symmetry and N peaks along ρ_z . This density structure can be regarded as a linear Wigner molecule. For $N=8$ the density phase is a CDW, with $N/2$ peaks along ρ_z and preserved spin symmetry. Instead, for $N=6$ the electron density presents an incipient SDW, with broken spin symmetry but with a ρ_z profile still showing $N/2$ maxima. Regardless of N , the distribution of the electron density is more pronounced near the rod caps [see dashed lines in Fig. 2(b)], in contrast with the situation held when harmonic potentials are used.³⁴

The comparison of the above situation with that displayed in Figs. 2, (a1)–(a3), for $\epsilon_{\text{out}}=1$ let us to conclude that the presence of an insulating environment does not alter in any case the electron correlation phase. The main effect of this environment is to push the electronic density toward the ends of the rod [see Fig. 2(b)], where ρ_z becomes significantly enhanced.

It is known that the presence of insulating external media tends to increase the electron-electron interaction and thus the electron correlation.^{9,20,35} This, together with the large anisotropy of the spatial and dielectric confinements in elongated QDs, leads us to expect substantial changes in the correlation phase experienced by the electrons in large NRs. However, we observe that the dielectric mismatch effect is not noticeable beyond the abovementioned increase in the electron density near the rod caps. Indeed, the normalized spin polarization $[(\rho_z^{\uparrow} - \rho_z^{\downarrow})/\max(\rho_z)]$, see Figs. 2, (c1)–(c3)] for $N=4$ and 6 shows a SDW that presents a similar antiferromagnetic modulation with similar maxima values both in the absence (dashed lines) and in the presence (solid lines) of dielectric discontinuities, despite the redistribution of ρ_z^{\uparrow} and

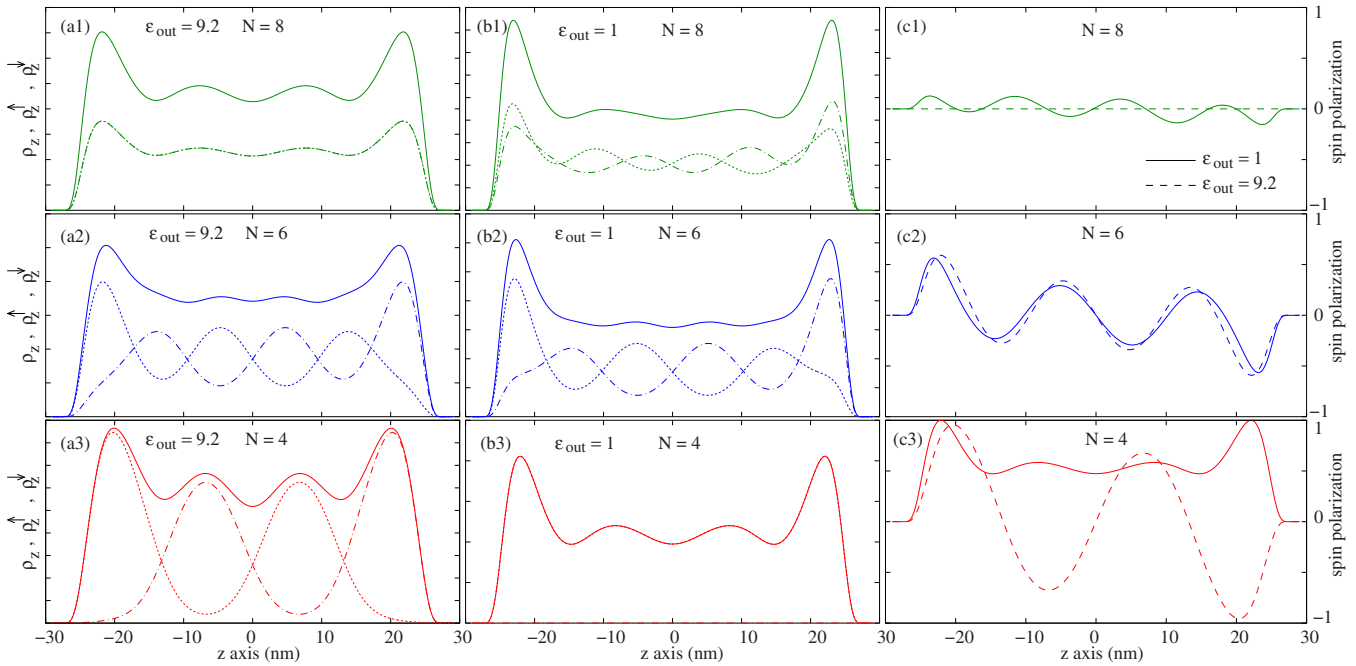


FIG. 3. (Color online) [(a1)–(a3)] ρ_z (solid), ρ_z^\uparrow (dotted), and ρ_z^\downarrow (dash dotted) densities for a $L=50$ nm CdSe rod immersed in a $\epsilon_{\text{out}}=9.2$ dielectric medium and populated with $N=8$, 6, and 4 electrons. [(b1)–(b3)] Same as above but for $\epsilon_{\text{out}}=1$. [(c1)–(c3)] Normalized spin polarization [$(\rho_z^\uparrow - \rho_z^\downarrow)/\max(\rho_z)$] for the studied cases assuming $\epsilon_{\text{out}}=1$ (solid lines) and $\epsilon_{\text{out}}=9.2$ (dashed lines).

ρ_z^\downarrow toward opposite ends of the rod. Although spin polarization is locally not zero, it yields a zero total spin, as it is an odd function of z [see Figs. 2, (c2)–(c3)].

By means of probing several L values (not shown) we have checked that the dilution of the electron density by increasing the rod length has a much more relevant effect on the stability of the ground state correlation phase than the increase in the electron–electron interactions induced by the external medium. Yet, in the vicinity of phase transitions this last effect can invert the order of stability of the phases involved. Although this effect is quite focalized, for the sake of illustration we include in Fig. 3, a similar comparison than that of Fig. 2 but for $L=50$ nm. We represent this time ρ_z , ρ_z^\uparrow , and ρ_z^\downarrow for both $\epsilon_{\text{out}}=9.2$ [Figs. 3, (a1)–(a3)] and $\epsilon_{\text{out}}=1$ [Figs. 3, (b1)–(b3)]. As we can observe, for $N=8$ the system presents a CDW in the absence of dielectric mismatch, preserving the spin symmetry and a null spin polarization [dashed line in Fig. 3, (c1)], but turns into an incipient SDW with breakdown of the spin symmetry for $\epsilon_{\text{out}}=1$ [see Fig. 3, (b1), and solid line in Fig. 3, (c1)]. As for $N=4$, the presence of the insulating medium yields a transition from the SDW to the fully polarized phase [see Figs. 3, (a3)–(c3)].³⁶ However, it must be pointed out that the LSDA energy differences among the phases discussed in each case ($N=4$ and 8) is lower than 1 meV.

IV. CONCLUDING REMARKS

In this paper, we propose a feasible model to account for the dielectric confinement in LSDA for arbitrarily shaped QDs. The model which has a good agreement with FCI calculations (including exact dielectric confinement) is then used to study the influence of the dielectric confinement on the electronic charge distribution of elongated QDs in the

low density regime. Insulating dielectric media yield a redistribution of the electron density toward the ends of few-electron colloidal NRs. Even in diluted density regimes, the onsets of the density phase transitions remain almost unaltered, and the spin polarization density wave of broken symmetry phases is not noticeably perturbed except in the vicinity of phase transitions.

ACKNOWLEDGMENTS

Continuous support from MCINN Project Nos. CTQ2008-03344 and FIS2008-00421, UJI-Bancaixa Project No. P1-1A2009-03, and Generalitat de Catalunya Project No. 2009SGR1289 are gratefully acknowledged.

- ¹J. D. Jackson, *Classical Electrodynamics* (Wiley, New York, 1962).
- ²R. Tsu, *Microelectron. J.* **34**, 329 (2003).
- ³A. Konar and D. Jena, *J. Appl. Phys.* **102**, 123705 (2007).
- ⁴D. Katz, T. Wizansky, O. Millo, E. Rothenberg, T. Mokari, and U. Banin, *Phys. Rev. Lett.* **89**, 086801 (2002).
- ⁵J. Wang, M. Gudiksen, X. Duan, Y. Cui, and C. Lieber, *Science* **293**, 1455 (2001).
- ⁶A. Lan, J. Giblin, V. Protasenko, and M. Kuno, *Appl. Phys. Lett.* **92**, 183110 (2008).
- ⁷K. Wu, K. Chu, C. Chao, Y. Chen, C. Lai, C. Kang, C. Chen, and P. Chou, *Nano Lett.* **7**, 1908 (2007).
- ⁸V. Barzda, R. Cisek, T. L. Spencer, U. Philipose, H. E. Ruda, and A. Shik, *Appl. Phys. Lett.* **92**, 113111 (2008).
- ⁹L. E. Brus, *J. Chem. Phys.* **79**, 5566 (1983); **80**, 4403 (1984).
- ¹⁰A. Shabaev and A. L. Efros, *Nano Lett.* **4**, 1821 (2004); S. F. Wuister, C. M. Donegá, and A. Meijerink, *J. Chem. Phys.* **121**, 4310 (2004); V. A. Fonoberov, E. P. Pokatilov, and A. A. Balandin, *Phys. Rev. B* **66**, 085310 (2002).
- ¹¹P. G. Bolcatto and C. R. Proetto, *J. Phys.: Condens. Matter* **13**, 319 (2001).
- ¹²J. L. Movilla and J. Planelles, *Comput. Phys. Commun.* **170**, 144 (2005).
- ¹³C. Xue and S. Deng, *Comm. Comp. Phys.* **8**, 374 (2010).
- ¹⁴J. L. Movilla, J. I. Climente, and J. Planelles, *Comput. Phys. Commun.* **181**, 92 (2010).
- ¹⁵D. Boda, D. Gillespie, W. Nonner, D. Henderson, and B. Eisenberg, *Phys.*

- ¹⁵*Rev. E* **69**, 046702 (2004).
- ¹⁶H. Hoshi, M. Sakurai, Y. Inoue, and R. Chûjô, *J. Chem. Phys.* **87**, 1107 (1987).
- ¹⁷J. M. Badia, M. Castillo, J. I. Clemente, M. Marqués, R. Mayo, J. L. Movilla, J. Planelles, and E. S. Quintana-Ortí, in Proceedings of the 10th International Conference on Computational and Mathematical Methods in Science and Engineering, J. Vigo-Aguilar, Ed. (Almeria, Spain, 2010), pp. 133–141.
- ¹⁸J. M. Badia, J. L. Movilla, J. I. Clemente, M. Castillo, M. Marqués, R. Mayo, E. S. Quintana-Ortí, and J. Planelles (unpublished).
- ¹⁹J. L. Movilla, J. Planelles, and W. Jaskólski, *Phys. Rev. B* **73**, 035305 (2006); J. L. Movilla and J. Planelles, *ibid.* **74**, 125322 (2006); **75**, 195336 (2007).
- ²⁰J. I. Clemente, M. Royo, J. L. Movilla, and J. Planelles, *Phys. Rev. B* **79**, 161301(R) (2009).
- ²¹R. G. Parr and W. Yang, *Density-Functional Theory of Atoms and Molecules* (Oxford University Press, Oxford, 1989).
- ²²J. Kainz, S. A. Mikhailov, A. Wensauer, and U. Rössler, *Phys. Rev. B* **65**, 115305 (2002).
- ²³S. M. Reimann and M. Manninen, *Rev. Mod. Phys.* **74**, 1283 (2002).
- ²⁴M. Pi, D. G. Austing, R. Mayol, K. Muraki, S. Sasaki, H. Tamura, and S. Tarucha, in *Trends in Quantum Dots Research*, edited by P. A. Ling (Nova Science, New York, 2005); D. G. Austing, S. Sasaki, K. Muraki, Y. Tokura, K. Ono, S. Tarucha, M. Barranco, A. Emperador, M. Pi, and F. Garcias, in *Nano-Physics & Bio-Electronics: A New Odyssey*, edited by T. Chakraborty, F. M. Peeters, and U. Sivan (Elsevier, New York, 2002).
- ²⁵M. Pi, M. Royo, and J. Planelles, *J. Appl. Phys.* **100**, 073712 (2006); M. Royo, J. Planelles, and M. Pi, *Phys. Rev. B* **75**, 033302 (2007).
- ²⁶W. Kohn and L. J. Sham, *Phys. Rev.* **140**, A1133 (1965).
- ²⁷J. Planelles, M. Royo, A. Ballester, and M. Pi, *Phys. Rev. B* **80**, 045324 (2009).
- ²⁸It is known that LSDA generally overestimates exchange and correlation in extremely diluted systems (see, e.g., Ref. 29). Then, the bit larger compression of the LSDA function may be related to this overestimation.
- ²⁹F. Pederiva, A. Emperador, and E. Lipparini, *Phys. Rev. B* **66**, 165314 (2002).
- ³⁰For an assessment of the dilute regime and Wigner molecules in one-dimensional and quasi-one-dimensional systems, see e.g. Refs. 27 and 31–33.
- ³¹W. Häusler and B. Kramer, *Phys. Rev. B* **47**, 16353 (1993).
- ³²E. Räsänen, H. Saarikoski, V. N. Stavrou, A. Harju, M. J. Puska, and R. M. Nieminen, *Phys. Rev. B* **67**, 235307 (2003).
- ³³B. Szafran, F. M. Peeters, S. Bednarek, T. Chwiej, and J. Adamowski, *Phys. Rev. B* **70**, 035401 (2004).
- ³⁴S. M. Reimann, M. Koskinen, and M. Manninen, *Phys. Rev. B* **59**, 1613 (1999).
- ³⁵A. Franceschetti, A. Williamson, and A. Zunger, *J. Phys. Chem. B* **104**, 3398 (2000); A. Orlandi, M. Rontani, G. Goldoni, F. Manghi, and E. Molinari, *Phys. Rev. B* **63**, 045310 (2001).
- ³⁶The real existence of the fully polarized phase should be taken with caution, in the sense that LSDA generally overestimates exchange and correlation in extremely diluted systems (see, e.g., Ref. 29).